Chapter 65
Sisal Fiber/Fly Ash-Reinforced Hybrid Polypropylene Composite: An Investigation into the Thermal, Rheological, and Crystallographic Properties

Atul Kumar Maurya, Rupam Gogoi, and Gaurav Manik

Abstract The current work aims to develop fly ash (FA) and sisal fiber-reinforced (SSL) polypropylene (PP) composites via injection molding. X-ray diffraction (XRD), differential scanning calorimetry (DSC), and rheology test were performed for evaluating crystallography, crystallinity, and melt viscosity. XRD study reveals the increase in β phase of the PP due to the addition of styrene-(ethylene-*co*-butylene)-styrene (SEBS) and maleic anhydride-grafted SEBS. This induced β phase increased further upon the addition of FA to the composite systems. β phase improved toughness and impact strength of the composites. DSC investigation revealed highest and lowest crystallinity of 43.46 and 17.49% for PP and composite made of 30 wt% of FA to the base matrix (BM). A decrease in crystallization temperature was observed for the BM and all the composites compared to PP. Rheological properties showed that at lower frequencies (rad/s), melt viscosity was governed by reinforcements (FA/SSL), and highest storage modulus of 297 MPa was recorded for 30 wt% SSL-reinforced BM composite. However, at higher frequencies (100 rad/s), BM recorded higher value of storage modulus than 30 wt% reinforced SSL/BM composites.

Keywords Hybrid composites · Eco-friendly · Rheology · Crystallography

Introduction

Use of synergistical properties of multiphase materials are in use since centuries due to many significant advantages [1, 2]. For instance, lightweight fiber-reinforced composites having enhanced specific mechanical properties compared to their

A. K. Maurya · R. Gogoi · G. Manik (✉)
Department of Polymer and Process Engineering, Indian Institute of Technology Roorkee, Saharanpur Campus, Paper Mill Road, Saharanpur, UP 247001, India
e-mail: gaurav.manik@pe.iitr.ac.in

A. K. Maurya
e-mail: amaurya@pe.iitr.ac.in

© The Author(s), under exclusive license to Springer Nature Singapore Pte Ltd. 2023

G. Manik et al. (eds.), *Recent Advances in Mechanical Engineering*, Lecture Notes in Mechanical Engineering, https://doi.org/10.1007/978-981-19-2188-9_65

conventional metallic counterparts have found applications in aircrafts and automotive. In particular, hollow glass microspheres used with carbon [3] and bamboo [1] fiber-reinforced PP hybrid composites prepared earlier offered high specific strength, low cost, and lightweight. Although these composites reported desirably high strength-to-weight ratio but were still far from environmental friendliness. Reinforcement of industrially useful natural fibers like sisal, flax, hemp, and kenaf to the polymer composites is trending now a days. For instance, use of flax fiber instead of carbon fiber in polymer composite for making formula one racing car seats designed by Bcomp and McLaren [4] has been reported to lower 75% CO_2 footprint. Another industrial fiber is sisal (SSL) which is robust, strong, and has specific strength comparable to their synthetic counterpart. Many literatures have already reported improved mechanical and thermomechanical properties of sisal fiber-reinforced PP, polyethylene, and epoxy composites [5] for the application of interior panels of air buses [2]. However, addition of stiff SSL fiber to the ductile and soft polymer leads to an undesirable reduction of the impact strength of the composites [1]. Addition of toughening agents like styrene-(ethylene-*co*-butylene)-styrene (SEBS) and ethylene propylene rubber to these composites could be an answer to counter-reduced impact strength. Another major drawback associated with natural fiber is its hydrophilic nature that provides weak interfacial adhesion at fiber/matrix interface and is prone to the moisture absorption. Simultaneous effect of procuring treatment of fiber and use of compatibilizer reported noticeable improvement in the mechanical properties and moisture mitigation of the composites [6]. Surface treatment and use of suitable coupling agents aids in improved fiber-matrix adhesion and, thereby, helps in suitably transferring load from base matrix to the reinforcements. Many treatments techniques like alkali, silane, and combined alkali–silane treatment simultaneously have already been reported. It is already reported by Panaitescu et al. that joined procure of NaOH and APTES treatment gives superior compatibility compared to using them alone [6].

Among the ample of wastes generated from the different industries, FA has most concerning issue for habitat and fauna life. Presence of heavy and dangerous metals like V, Cd, Ni, and Cr may contaminate the groundwater. Hence, deployment of FA is a major problem across the globe. However, the presence of suitable inorganic components like silicates (SiO_2) and aluminates (Al_2O_3) makes FA a potential filler for reinforcing in polymers.

However, just like natural fibers, low compatibility at the interface of the FA filler and matrix too results in poor mechanical properties. In this direction, the highest mechanical properties of FA/thermoplastic polymer composite were reported for FA diameter not more than 45 μm, APTES treatment, and loading not more than 15 wt% [7]. Recently reported FA filled banana fiber, and recycled PE hybrid composite showed an increase in mechanical properties and resistance against water absorption [8].

The current study employs FA/SSL/PP hybrid composites. An optimized blend of 85 wt% PP, 10 wt% SEBS (toughening agent), and 5 wt% SEBS-g-MA (coupling agent) was used as base matrix (BM). Hybridization of FA particles with SSL/BM showed an improvement in mechanical properties and resistance against moisture

absorption of the composites as reported in our previous study [1]. However, the effect of FA particles, SEBS, and SEBS-g-MA on the rheological, crystallographic, and thermal properties of the composites remains unexplained. Hence, investigation and evaluation of viscosity from rheology, thermal behavior from differential scanning calorimetry (DSC), and crystallography from X-ray diffraction (XRD) of such interesting composites has been reported here.

Materials, Methods, and Experiments

Materials

Isotactic polypropylene (HY-110 MA) from Reliance India, MA-g-SEBS (Beiwa® 901) from DZBH New Materials China, SEBS (Kraton G1651 H) with styrene to rubber ratio 33:67 from KRATON Corporation USA, and FA (Fillit™ 500s) from Petra India were obtained from their respective companies. 3-Aminopropyltriethoxysilane (APTES) and sodium hydroxide (NaOH) were obtained from Sigma-Aldrich. SSL fibers were purchased from a local vendor.

Methods

Base matrix preparation
BM was selected as matrix on the behalf of various properties including tensile, flexural, and notched impact strength. Enhanced notched impact strength by the proposed BM was reported earlier in our previous study, along with interfacial adhesion between reinforcing fiber/filler and BM. Proposed BM constitutes of 85 wt% PP, 10 wt% SEBS (elastomer), and 5 wt% of MA-g-SEBS (compatibilizer) were optimized, and have, selected as the BM, similar to those used in the previous work [2]. Rheomix QC Lab compounder was used for mixing the polymer, elastomer, and coupling agent for appropriate time to achieve an uniform blend of the various components.

Reinforcing Fiber
SSL fiber as received was laundered under running water, sun dried, and treated with 1% (*w*/*w*) of NaOH at 80 °C followed by 2% (*w*/*w*) APTES coating on the fiber surface. Thereafter, 4 mm length of NaOH-APTES-treated SSL fibers was ready to use for formulating the composites. A detailed treatment process, temperature, and drying precautions have already been explained in our previous paper [1, 9].

Reinforcing Filler FA
FA particles were grounded in a single ball mill, and the reduced size was confirmed from dynamic light scattering. The reduced FA particles (~2 μm) were then silane

treated with 1 wt% of APTES dissolved in 90:10 (*w/w*) ethyl alcohol and water solution at ambient temperature for 1 h. Silane-treated FA has been filtered and kept in a hot oven for drying purposes. After drying for more than 12 h. at 100 °C, received chunks of the oven-dried FA were ball milled again to break the lumps.

BM and composite fabrication

The polymer, elastomer, comtabilizer, and NaOH-APTES procured SSL/FA were dried prior at 80 °C in an oven prior to mixing/compounding. Thereafter, a blend of 85 wt% PP, 10 wt% SEBS, and 5 wt% MA-g-SEBS has been selected as BM which was already optimized and used successfully in our previous work [2]. Different composites were then formulated as 30 wt% SSL in PP (Co-1), 30 wt% SSL in BM (Co-2), and 30 wt% FA in BM (Co-3). For hybrid composites, FA content was increased from 5–15 wt% with proportional decrease in SSL from 30–15 wt% in Co-2 and named as Hy-1, Hy-2, and Hy-3.

PP, SEBS, and coupling agent MA-g-SEBS were fed into the hopper of HAAKE™ Rheomix QC Lab Mixer (Make; ThermoFisher SCIENTIFIC) for polymer blend preparation. The machine's temperature and screw speed were maintained between 185–190 °C at 10–50 rpm.

To avoid any possible agglomeration of the silane-treated SSL and FA, both the reinforcements were added slowly and separately to the melt blend of the BM. The composite mixture obtained from the Rheomix was melted and compounded again in micro-compounder HAAKE™ MiniCTW (Make; ThermoFisher SCIENTIFIC). The temperature and screw speed were maintained between 185–190 °C at 50 rpm. This molten mixture was then relocated to the chamber of the HAAKE™ Minijet II for pushing the melt mix to the mold of the samples maintained at around 60 °C.

Testing and Characterization

X-ray Diffraction

Rigaku Ultima IV (Make:Japan) instrument was used for XRD characterization to investigate any crystallographic and planar changes in the PP, BM, and composites. Samples were scanned in the range of 5° to 30° from a Cu-k_α source at 40 kV and 40 mA.

Differential Scanning Calorimetry (DSC)

The DSC was carried out using TA instrument (Discovery series DSC 25) setup as per ASTM D3418-15 standard. PP, BM, and composite samples were placed in a crucible and exposed to heating and cooling cycles (minimum 2) within a temperature

range of −60 °C to 250 °C with 10 °C/min heating rate under a nitrogen atmosphere. Samples were heated/cooled in three cycles starting from room temperature to 250 °C (heating), 250 °C to −60 °C (cooling), and final −60 °C to 250 °C (heating). Percent crystallinity of the composites and pristine samples have been determined by the following formula:

$$\%X_c = \frac{\Delta H}{\Delta H^*} \times 100 \tag{65.1}$$

ΔH and ΔH^* are the melting enthalpies of samples and 100% crystalline PP. The value of ΔH^* has been selected as 209 J/g for this experiment as per earlier reports in literature [10].

Rheology Analysis

A circular disk-type sample with a 25 mm diameter was used in a MC102 rheometer (Anton Paar, Australia) to investigate viscoelastic behavior of the composites. Parallel plates with 25 mm diameter and a gap of 1.5 mm were used for the analysis. Samples were scan in a range of 0.1–100 rad/s at 180 °C within the viscoelastic region.

Results and Discussions

XRD Analysis

Crystallographic study of the PP, BM, and all the composites was investigated by using XRD techniques, and different curves have been reported in Fig. 65.1. Various crystallographic planes corresponding to 2θ value have been shown in the figure. Change in peak height is reported in Table 65.1. For instance, peaks corresponding

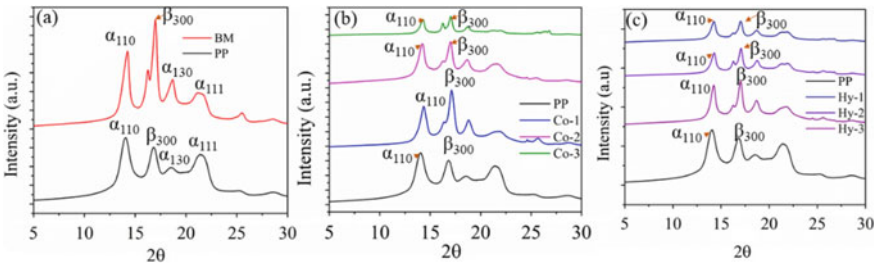

Fig. 65.1 XRD plot of PP versus **a** BM, **b** Composites, **c** hybrid composites

Table 65.1 Details of crystallization and melting temperature, melting enthalpy and percentage crystallinity of pristine PP, base matrix, and fabricated composites

Samples	T_c/°C	T_m/°C	ΔH (J/g)	% X_c
PP	121.44	163.62	90.85	43.46
BM	112.47	161.13	67.65	32.36
Co-1	114.94	160.21	54.66	26.15
Co-2	117.37	158.96	43.81	20.96
Co-3	114.26	162.69	36.57	17.49
Hy-1	116.01	158.01	46.79	22.38
Hy-2	116.12	157.25	43.20	20.66
Hy-3	115.83	115.40	43.69	20.90

to 2θ value 14.24°, 16.85°, 18.55°, and 21.47 represent α_{110}, β_{300}, α_{130}, and α_{111} planes of the PP [1], respectively. Peak at 300 planes is due to the β phase which is the characteristic peak for the PP and already reported earlier by Gogoi et al. [1]. It was presumed that β phase of the composites is induced due to the input of heterogeneous nucleation from FA and SSL. Noticeably, from Fig. 65.1a, in isotactic PP, α phase is more than β phase region for the crystalline nature of the PP. However, addition of SEBS and SEBS-g-MA to PP increases the β phase and decreases the α phase attributed to the heterogeneous nucleation of the PP. Hence, as a result, due to the presence of β crystal, improved toughness, elongation at break, and impact strength of the BM have been achieved [1]. Likewise, such heterogeneous nucleation has been reported to improve processability of the composites in injection molding [1].

Figure 65.1a shows the comparative study of α_{110} and β_{300} peaks between pristine PP and composites Co-1, Co-2, and Co-3. Clearly, there is increase in the β_{300} peak of all the composites exhibited due to the heterogeneous nucleation around the SSL fiber. However, it was presumed that Co-2 and Co-3 will exhibit much improved toughness (due to β phase) compared to Co-1 due to the presence of SEBS and SEBS-g-MA in them. Likewise, Fig. 65.1c depicts the α_{110} and β_{300} peaks of the hybrid composites Hy-1, Hy-2, and Hy-3. A significant change in the peak height of β_{300} is due to the addition of FA and SSL fiber. A shoulder can also be observed just beside the β_{300} peak and increases with the increment of the FA content. From the above discussion, it can be concluded that the addition of SEBS and SEBS-g-MA, along with FA, increased the overall toughness of the composites. It was presumed that increase of β phase must decrease the percentage crystallinity of the composites. The effect on crystallinity of the composites has been discussed in the next section.

DSC

Figure 65.2a, b represent the crystallization and melting curves of the various samples against the temperature. Respective temperature at maximums of exothermic curve from cooling cycle and endothermic curve from second heating cycles was taken as the crystallization (T_c) and melting temperature (T_m). T_c of the pristine PP was recorded at around 121 °C which was in agreement with the literature reported earlier [11]. However, addition of SEBS and SEBS-g-MA to the PP resulted in the reduction of the T_c due to the heterogeneity induced due to higher crystallization rate from SEBS and SEBS-g-MA particles. It was also expected that mere presence of these particles leads to the imperfect crystallization of the PP, and T_c was found to be 112 °C and which was in agreement with Satapathy et al. [8]. Interestingly, T_c of Co-1, Co-2, Co-3, Hy-1, Hy-2, and Hy-3 was found to be 114 °C, 117 °C, 114.26 °C, 116.01 °C, 116.12 °C, and 115.83 °C, respectively. Addition of 30 wt% SSL fiber to the BM increased the T_c by 5 °C compared to BM. This increment might be attributable to the heterogeneous nucleating effect of SSL fiber which eventually accelerated the crystallization rate and pushed the T_c at higher temperature. This increment of T_c was also recorded for the subsequent addition of 5–15 wt% of FA to the hybrid composites Hy-1, Hy-2, and Hy-3. It is worth mentioning that induced heterogeneity for spherulite nucleation of the SSL and FA was almost equivalent and exhibited the T_c of all the composites in between BM and PP. It is also reported that decrease in peak temperature of T_c implies an increase in supercooling [11].

In Fig. 65.2a, the melting peak T_m of PP showed a single peak around 163 °C, which was due to the presence of majority of α phase [1]. Likewise, BM, Co-1, Co-2, Co-3, Hy-1, Hy-2, and Hy-3 showed major peak at around 150–155 °C with a shoulder at 163 °C (α phase) exhibited due to the increment in the tough β phase of the BM and all the composites [12].

Inclusion of SEBS, SEBS-g-MA, SSL, and FA was presumed to increase β phase crystallinity of the PP as already explained in Sect. "XRD Analysis". Consequently, a decrease in the ΔH and X_c of BM and all the composites were recorded compared to PP. This decrease in crystallinity was exhibited due to the restriction in spherulite

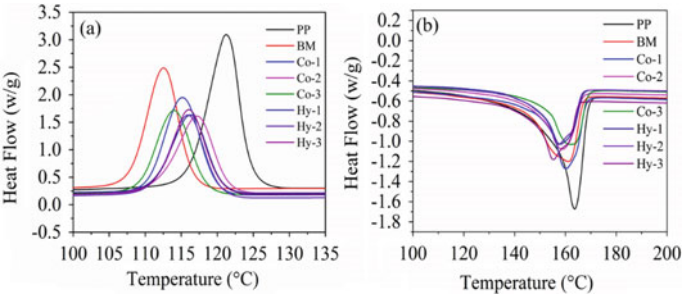

Fig. 65.2 Thermogram of PP versus rad/s BM, **b** Composites, **c** hybrid composites

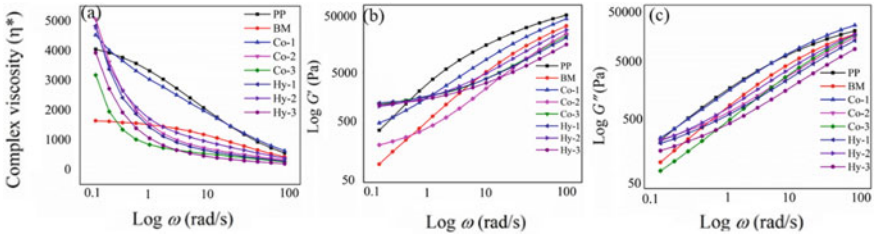

Fig. 65.3 Illustration of rheology of PP versus BM, composites, and hybrid composites expressed in terms of complex viscosity, storage, and loss modulus against angular frequency

growth along the lateral direction and resulting in a columnar layer [8]. Table 65.1 represents the T_c, T_m, ΔH, and X_c of PP, BM, and all the composites.

Rheology

Rheological properties of the PP and various samples of the composites were studied in a frequency sweep test at 180 °C in linear viscoelastic regime (LVE). Test was carried out at a fixed strain rate of 1% from 0.1 to 100 rad/s. Figure 65.3a–c represents the complex viscosity (η^*), storage (G'), and loss modulus (G'') versus frequency (ω) of the samples.

Figure 65.3a, pristine PP, shows a shear thinning behavior beyond frequency ($\omega > 1$), and this was in agreement with the data reported earlier by Gogoi et al. [13]. BM and all the composites follow the same flow behavior as that of PP. Addition of SEBS and SEBS-g-MA reduces the η^* of the BM due to the lower viscosity of these components itself; addition of olefins decreases the viscosity thereby improving the processability characteristics. The BM shows a plateau in the viscosity value at lower frequencies indicating that disentanglement of polymer chains occurs so slowly that the recoiling of polymer chains occurs at the similar rate due to which viscosity remains constant. Moreover, larger differences were observed at lower frequencies when olefins added to the PP; since at lower frequencies, the imprints of the polymeric chains or network were more visible as it gets longer time to get relax. On contrary to this, addition of fiber/filler to the matrices PP and BM increased the η^* of the Co-1, Co-2, Co-3, Hy-1, Hy-2, and Hy-3. This increase in viscosity was exhibited due to the obstruction in flow created by filler/fiber at lower frequencies. Co-1 which constitutes 30 wt% of SSL fiber in PP shows higher η^* compared to PP at lower frequencies and almost equivalent or marginally higher at higher frequencies. However, inclusion of SEBS and SEBS-g-MA reduces the η^*, and same has been reported earlier [14]. Interestingly, Co-2 and Co-3 showed highest and lowest η^* values and η^* among all the other hybrid composites. Moreover, presence of spherical ball type and planar flake type of FA which act as an effective ball-bearing element and increased the

Table 65.2 Values of storage and loss modulus at $\omega = 0.1$ and 100 rad/s

Samples	G'		G''	
	0.1 (rad/s)	100 (rad/s)	0.1 (rad/s)	100 (rad/s)
PP	66.40	55,500	403	35,500
BM	9.19	29,500	164	30,600
Co-1	102	44,800	442	44,100
Co-2	297	16,500	410	26,900
Co-3	28.2	18,900	116	29,500
Hy-1	327	14,700	356	23,500
Hy-2	268	23,400	396	30,400
Hy-3	291	9990	263	16,700

segmental chain mobility, and hence, reduce the viscosity of Co-3 compared to Co-2 [13, 15]. It is also worth mentioning that increase in SSL content increases the melt viscosity of the samples, especially at lower frequencies. However, at higher frequencies, η^* of all the composites decreases drastically and went down to value close to that of BM. At $\omega = 100$ rad/s, highest η^* was recorded for the BM. It is worth mentioning that at lower frequencies, viscosity is governed by reinforcements and interaction between fiber/matrix, while at higher frequencies, it is governed by matrix. Hence, as a result, at higher frequencies due to fiber alignment, layered flow/slip develops among each layer, and simultaneous effect of shear rate from each layer was much higher than the macroscopic shear rate [13]. Some literatures have also been reported that treatment of reinforcement with silane coupling agent also reduces the viscosity of the samples.

G' and G'' followed the same trend as of η^*. Increase in the values of G' and G'' of composites was recorded with increasing SSL content, whereas these decreased with an increase of frequency. Table 65.2 depicts the value of G' and G''. It can be observed that at 0.1 rad/s, greatest and lowest G' were demonstrated for hybrid composite Hy-1 and BM. This is in the agreement with the similar effect reported earlier by Gogoi et al. [1].

As frequency increases, a decrease in G' has been recorded. This was in accordance with the η^*, where at lower frequencies, viscosity was higher and decreased at higher frequencies even down to BM. Likewise, G'' which is the measure of the heat dissipation was highest for the Co-1 and lowest for the Co-3. This also confirms that the heat absorbed by the SSL fiber was more than that of the FA.

Conclusions

In the present work, a synergistic effect of FA and SSL fiber on SEBS and SEBS-g-MA-toughened PP composite has been reported. XRD report confirms a change

in crystallinity due to the addition of SEBS and SEBS-g-MA to the PP. In isotactic PP, where α phase is major, addition of these toughening agents induces β phase crystallinity in the BM. Presence of this β phase in BM is the key reason behind the improved toughness, elongation, and impact strength. Likewise, inclusion of FA and SSL induces β phase crystallinity due to the heterogeneous nucleation. DSC thermogram was in accordance with the same. Highest α crystallinity of 43.46% was reported for PP compared to BM and all other composites. The decrease in crystallinity was due to the imperfect crystal packing and presence of heterogeneity. Rheological properties showed increment in the complex viscosity, storage, and loss modulus with the inclusion of FA/SSL reinforcement. However, at higher frequencies, these values decreased and came down to that of BM. Conclusively, plasticizing effect of FA particles at higher frequencies is prominent as compared to lower frequencies. As a result, G' of all the hybrid composites was higher than that of the PP and BM.

References

1. Gogoi R, Kumar N, Mireja S et al (2019) Effect of Hollow glass microspheres on the morphology, rheology and crystallinity of short bamboo fiber-reinforced hybrid polypropylene composite. JOM 71:548–558. https://doi.org/10.1007/s11837-018-3268-3
2. Maurya AK, Gogoi R, Manik G (2021) Study of the moisture mitigation and toughening effect of fly-ash particles on sisal fiber-reinforced hybrid polypropylene composites. J Polym Environ 1–16. https://doi.org/10.1007/s10924-021-02043-3
3. Gogoi R, Manik G, Arun B (2019) High specific strength hybrid polypropylene composites using carbon fibre and hollow glass microspheres: development, characterization and comparison with empirical models. Compos Part B Eng 173:106875. https://doi.org/10.1016/j.compositesb.2019.05.086
4. McLaren's Formula One Car Features Natural Fiber Composite Seat | Composites Manufacturing Magazine. http://compositesmanufacturingmagazine.com/2020/08/mclarens-formula-one-car-features-natural-fiber-composite-seat/. Accessed 13 Mar 2021
5. Jain S, Das R, Ramachandran M (2020) Review on Mechanical, Thermal and Morphological Characterization of Sisal Fibre Composite. In: IOP Conference Series: Materials Science and Engineering. Institute of Physics Publishing, p 012074
6. Panaitescu DM, Vuluga Z, Sanporean CG et al (2019) High flow polypropylene/SEBS composites reinforced with differently treated hemp fibers for injection molded parts. Compos Part B Eng 174:107062. https://doi.org/10.1016/j.compositesb.2019.107062
7. Ares A, Pardo SG, Abad MJ et al (2010) Effect of aminomethoxy silane and olefin block copolymer on rheomechanical and morphological behavior of fly ash-filled polypropylene composites. Rheol Acta 49:607–618. https://doi.org/10.1007/s00397-009-0417-1
8. Satapathy S, Kothapalli RVS (2018) Mechanical, dynamic mechanical and thermal properties of banana fiber/recycled high density polyethylene biocomposites filled with flyash cenospheres. J Polym Environ 26:200–213. https://doi.org/10.1007/s10924-017-0938-0
9. Maurya AK, Gogoi R, Manik G (2021) Mechano-chemically activated fly-ash and sisal fiber reinforced PP hybrid composite with enhanced mechanical properties (in press)
10. Cui YH, Wang XX, Li ZQ, Tao J (2010) Fabrication and properties of nano-ZnO/glass-fiber-reinforced polypropylene composites. J Vinyl Addit Technol 16:189–194. https://doi.org/10.1002/vnl.20231

11. Gupta AK, Purwar SN (1984) Crystallization of PP in PP/SEBS blends and its correlation with tensile properties. J Appl Polym Sci 29:1595–1609. https://doi.org/10.1002/app.1984.070290514
12. Kulkarni MB, Radhakrishnan S, Samarth N, Mahanwar PA (2019) Structure, mechanical and thermal properties of polypropylene based hybrid composites with banana fiber and fly ash. Mater Res Express 6:075318. https://doi.org/10.1088/2053-1591/ab12a3
13. Gogoi R, Manik G (2021) Development of thermally conductive and high-specific strength polypropylene composites for thermal management applications in automotive. Polym Compos pc.25947. https://doi.org/10.1002/pc.25947
14. Su F-H, Huang H-X (2009) Mechanical and rheological properties of PP/SEBS/OMMT ternary composites. J Appl Polym Sci 112:3016–3023. https://doi.org/10.1002/app.29875
15. Parvaiz MR (2012) Influence of silane-coupling agents on the performance of morphological, mechanical, thermal, electrical, and rheological properties of polycarbonate/fly ash composites. Polym Compos 33:1798–1808. https://doi.org/10.1002/pc.22325